

A LOCAL LEVEL SET METHOD FOR PARAXIAL GEOMETRICAL OPTICS*

JIANLIANG QIAN[†] AND SHINGYU LEUNG[†]

Abstract. We propose a local level set method for constructing the geometrical optics term in the paraxial formulation for the high frequency asymptotics of two-dimensional (2-D) acoustic wave equations. The geometrical optics term consists of two multivalued functions: a travel-time function satisfying the eikonal equation locally and an amplitude function solving a transport equation locally. The multivalued travel-times are obtained by solving a level set equation and a travel-time equation with a forcing term. The multivalued amplitudes are computed by a new Eulerian formula based on the gradients of travel-times and takeoff angles. As a byproduct the method is also able to capture the caustic locations. The proposed Eulerian method has complexity of $O(N^2 \log N)$, rather than $O(N^4)$ as typically seen in the Lagrangian ray tracing method. Several examples including the well-known Marmousi synthetic model illustrate the accuracy and efficiency of the Eulerian method.

Key words. paraxial eikonal equations, level sets, multivalued geometrical optics, caustics

AMS subject classifications. Primary 54C40, 14E20; Secondary 46E25, 20C20

DOI. 10.1137/030601673

1. Introduction. Geometrical optics is the branch of optics which is characterized by the neglect of the wavelength, i.e., that corresponding to the limiting case (wavelength) going to zero (*short wavelength*), or, equivalently, for the wave number near infinity (*high frequency*), since in this approximation the optical laws may be formulated in the language of geometry [5]. This definition is based on short wavelength assumption of light and can be generalized to deal with other wave phenomena as well. The linear or nonlinear partial differential equations describing these wave propagations involve a parameter, such as the wavelength λ , which is small compared to all other lengths in the problem [48]. The asymptotic method is for the asymptotic solution of PDEs governing these wave propagations.

Consider the linear acoustic wave equation. According to the Debye procedure, inserting the high frequency asymptotic ansatz into the wave equation reduces the resolution of the PDE into the resolution for a sequence of ODEs. Among all the terms in the asymptotic ansatz, the most important term is the zeroth order term, the so-called geometrical optics term [25]. The geometrical optics term consists of two functions, a phase function satisfying the eikonal equation, a first-order nonlinear PDE, and an amplitude function solving a linear transport equation with the phase gradient as coefficients. Thus to construct the geometrical optics term the eikonal equation has to be solved first for the phase function; then the transport equation for amplitude might be integrated afterwards.

Conventionally, the eikonal equation was solved by the method of characteristics, aka. the ray tracing method in the seismology and optics; thus the method inherits the intrinsic shortcoming of the Lagrangian method, i.e., the nonuniform resolution in the desired computational domain [8]. In this setup, the amplitude function could be obtained by solving an ODE system as well, and it has the similar shortcoming

*Received by the editors November 4, 2003; accepted for publication (in revised form) September 22, 2005; published electronically March 3, 2006. This research was supported by ONR grant N00014-02-1-0720.

[†]<http://www.siam.org/journals/sisc/28-1/60167.html>

[†]Department of Mathematics, UCLA, Los Angeles, CA 90095-1555 (qian@math.wichita.edu, syleung@math.ucla.edu).

[8]. Certainly it is possible to overcome this drawback by introducing complicated interpolation and bookkeeping data structures [46]. However, in the late 80's Vidale [45], and van Trier and Symes [44] introduced direct discretizations of the eikonal equation based on finite difference schemes, which are Eulerian approaches and yield uniform resolutions of the solution in the computational domain. As pointed out in [44], the obtained solution should be understood as the minimum phase or the first-arrival travel-time in the viscosity solution sense for Hamilton–Jacobi equations [26, 11]. Once the travel-time is obtained, the transport equation for amplitude might be integrated [49, 42, 35]. Since the viscosity solution usually develops kinks, the gradient of the phase function is discontinuous. Therefore, the resulting solution for the transport equation has to be understood in the measure sense [15]. The difference between the ray tracing solution and the finite difference solution of the eikonal equation is that one is multiple-valued and the other single-valued [3, 13]. Although the viscosity concept and related numerical methods provide a natural Eulerian framework for geometrical optics, the drawback is that it provides only first arrivals while some applications may require all arrival times. Moreover, White [47] proved that there is a high probability for so-called transmission caustics to occur in an inhomogeneous medium. Beyond transmission caustics, more than one ray passes over each point in space so that the phase is multivalued. Therefore, it is important to design Eulerian methods for multivalued solutions of the eikonal equation, in general, the Hamilton–Jacobi equation.

In the last decade or so, there have been a lot of efforts in this direction: geometrical domain decomposition type methods [2], slowness matching method [40, 41], dynamic surface extension method [37, 36], segment projection method [14], level set method [29, 33, 24, 10, 34], and phase space method [17]. See [3, 13] for up-to-date reviews of the above methods and moment-based methods [12, 19, 23, 20].

In this work we present a local level set method for paraxial geometrical optics. By paraxial we mean that the wave propagation has a spatial orientation so that one of the spatial directions may be viewed as an evolution direction. This criterion may be quantified by assuming a subhorizontal condition for the eikonal equation [41]. In [34], we presented a global level set method for the paraxial eikonal equation in the two-dimensional (2-D) case, and the computed multivalued travel-time matched the ray tracing solution very well even in the difficult synthetic Marmousi model. Therefore we proceed along the same line and design a fast local level set method for both multivalued travel-times and amplitudes, thus constructing the geometrical optics term. This construction will be useful for modern high resolution seismic imaging [18, 21, 39, 7, 28]. Our formulation for computing multivalued amplitude is based upon a level set formulation and an extension of the Eulerian amplitude formulation used in [35], which is different from the one used in [29]. As a byproduct, our formulation also yields the cuspidal caustic curves (A_3 type) [43], which is related to the catastrophe theory; thus it suggests that the level set theory can be used to study the catastrophe development. See [4] for another Eulerian method for capturing caustics. The overall complexity of our level set method is $O(N^2 \log N)$ rather than $O(N^4)$ as typically seen in the ray tracing formulation.

The rest of the paper is organized as follows: section 2 presents very briefly the paraxial formulation of the eikonal equation and the level set formulation for wavefront locations, travel-times, amplitudes and caustics; section 3 gives implementation details of the current formulation using the local level set method; section 4 shows some numerical examples to illustrate the efficiency and accuracy of the Eulerian method; and section 5 indicates some possible future works.

2. Governing equations.

2.1. Paraxial formulation for the eikonal equation. Consider a point source condition for the eikonal equation defined in an open, bounded domain

$$(1) \quad \Omega = \{(x, z) : x_{\min} \leq x \leq x_{\max}, 0 \leq z \leq z_{\max}\}.$$

To emphasize the point source condition the eikonal equation is written as follows,

$$(2) \quad |\nabla_{\mathbf{x}} \tau(\mathbf{x}, \mathbf{x}_s)| = \frac{1}{c(\mathbf{x})}.$$

$$(3) \quad \lim_{\mathbf{x} \rightarrow \mathbf{x}_s} \frac{\tau(\mathbf{x}, \mathbf{x}_s)}{\|\mathbf{x} - \mathbf{x}_s\|} = \frac{1}{c(\mathbf{x}_s)}, \quad \tau \geq 0,$$

where \mathbf{x}_s is the given source point.

In some applications, for example, wave propagation in reflection seismics, the travel-times of interest are carried by the so-called subhorizontal rays [21, 39, 35], where subhorizontal means *oriented in the positive z-direction*. By the method of characteristics for the eikonal equation (2), the point source condition (3) and the subhorizontal condition, we use depth z as the running parameter so that we have a reduced system [34]

$$(4) \quad \frac{dx}{dz} = \tan \theta$$

$$(5) \quad \frac{d\theta}{dz} = \frac{1}{c} \left(\frac{\partial c}{\partial z} \tan \theta - \frac{\partial c}{\partial x} \right)$$

with

$$(6) \quad x|_{z=0} = x_s$$

$$(7) \quad \theta|_{z=0} = \theta_s,$$

where θ_s varies from $-\theta_{\max} \leq \theta \leq \theta_{\max} < \frac{\pi}{2}$. In addition, the travel-time is computed by integrating

$$(8) \quad \frac{dt}{dz} = \frac{1}{c \cos \theta}$$

with

$$(9) \quad t|_{z=0} = 0.$$

2.2. Level set equation for wavefronts. If we define $\phi = \phi(z, x, \theta)$ such that the zero level set, $\{(x(z), \theta(z)) : \phi(z, x(z), \theta(z)) = 0\}$, gives the location of the reduced bicharacteristic strip $(x(z), \theta(z))$ at z , then we may differentiate the zero level set equation with respect to z to obtain

$$(10) \quad \phi_z + u\phi_x + v\phi_\theta = 0$$

with

$$(11) \quad u = \frac{dx}{dz} \text{ and } v = \frac{d\theta}{dz},$$

which are given by the ray equations (4-5). In essence, we embed the ray tracing equations as the velocity field, $\mathbf{u} = (u, v)$, into the level set equation which governs the motion of the bicharacteristic strips in the phase space.

The initial condition for the level set motion equation (10) is taken to be

$$(12) \quad \phi|_{z=0} = \phi(0, x, \theta) = x - x_s,$$

which is obtained from initial conditions (6) and (7). This is a signed distance function, satisfying $|\nabla_{x,\theta}\phi| = 1$, to the initial phase space curve

$$(13) \quad \{(x, \theta) : x = x_s, -\theta_{\max} \leq \theta \leq \theta_{\max}\}$$

in the reduced phase space

$$(14) \quad \Omega_p = \{(x, \theta) : x_{\min} \leq x \leq x_{\max}, -\theta_{\max} \leq \theta \leq \theta_{\max}\}.$$

Using the same boundary condition as in [34], we have

$$(15) \quad \left. \frac{\partial \phi}{\partial \mathbf{n}} \right|_{\partial \Omega_p} = 0$$

where \mathbf{n} is the outward normal along the boundary of Ω_p .

2.3. Travel-time. To determine the travel-time of the ray from the above level set equation, we now derive a corresponding equation governing the evolution of travel-time. By the subhorizontal condition in the paraxial formulation and the ray equation (8), let $F_{\mathbf{u}}(x, \theta; z)$ be the flow generated by the velocity field \mathbf{u} in the phase space (x, θ) along the z -direction. Thus we can write

$$(16) \quad \frac{dT}{dz}(z, F_{\mathbf{u}}(x, \theta; z)) = \frac{1}{c \cos \theta}.$$

Therefore, having $t = T(z, x, \theta)$, we get the following advection equation:

$$(17) \quad \frac{dt}{dz} = \frac{dT}{dz} = T_z + uT_x + vT_\theta = \frac{1}{c \cos \theta}.$$

The initial condition for T is specified according to the initial condition (9):

$$(18) \quad T|_{z=0} = T(0, x, \theta) = 0,$$

which is consistent with the initial condition (12).

Following the same argument as in [34], we use the boundary condition

$$(19) \quad \frac{\partial T}{\partial x} = \frac{1}{c \sin \theta},$$

on $x = x_{\min}$ and $x = x_{\max}$, and

$$(20) \quad \frac{\partial T}{\partial \theta} = \left(\sin \theta \frac{\partial c}{\partial z} - \cos \theta \frac{\partial c}{\partial x} \right)^{-1},$$

on $\theta = -\theta_{\max}$ and $\theta = \theta_{\max}$.

2.4. Amplitude. The amplitude of a ray can be computed according to the formula given in [49, 35]:

$$(21) \quad \tilde{A}(x, z; x_s, z_s) = \frac{1}{2\pi} \sqrt{\frac{c}{2}} \sqrt{|\nabla \tilde{T} \times \nabla \tilde{\psi}|},$$

where \tilde{T} and $\tilde{\psi}$ are, respectively, the travel-time and the takeoff angle of a ray reaching (x, z) from (x_s, z_s) . Travel-times and takeoff angles are well defined on each solution branch in the physical space (x, z) . To compute this quantity in the reduced phase space, we consider T as the extension of \tilde{T} to the phase space; furthermore, we may also extend $\tilde{\psi}$ and \tilde{A} to ψ and A in the (z, x, θ) space, respectively. Since the takeoff angle is constant along a given ray in the phase space, we have

$$(22) \quad \psi_z + u\psi_x + v\psi_\theta = 0.$$

Moreover, we have

$$(23) \quad \begin{aligned} \frac{\partial \tilde{T}}{\partial x} &= T_x + T_\theta \frac{\partial \theta}{\partial x}, \\ \frac{\partial \tilde{T}}{\partial z} &= T_z + T_\theta \frac{\partial \theta}{\partial z}, \\ \frac{\partial \tilde{\psi}}{\partial x} &= \psi_x + \psi_\theta \frac{\partial \theta}{\partial x}, \\ \frac{\partial \tilde{\psi}}{\partial z} &= \psi_x + \psi_\theta \frac{\partial \theta}{\partial z}. \end{aligned}$$

It follows that

$$(24) \quad \left| \nabla \tilde{T} \times \nabla \tilde{\psi} \right| = \left| (T_x \psi_\theta - T_\theta \psi_x) \left(-v + u \frac{\partial \theta}{\partial x} + \frac{\partial \theta}{\partial z} \right) - \frac{1}{c \cos \theta} \left(\psi_x + \psi_\theta \frac{\partial \theta}{\partial x} \right) \right|.$$

Since $\phi(z, x, \theta(x, z)) = 0$ on the zero level set and equation (5), we have

$$(25) \quad \frac{\partial \theta}{\partial x} = -\frac{\partial \phi / \partial x}{\partial \phi / \partial \theta} \quad \text{and} \quad \frac{\partial \theta}{\partial z} = v - u \frac{\partial \theta}{\partial x}.$$

Finally we have

$$(26) \quad A(z; x, \theta) = \frac{1}{2\pi} \sqrt{\frac{c}{2 \cos \theta}} \sqrt{\left| \frac{\psi_x \phi_\theta - \psi_\theta \phi_x}{\phi_\theta} \right|}.$$

To compute the amplitude, we need the derivatives of the level set function at different z 's. However, as illustrated in [34], reinitialization of the level set function is necessary and, unfortunately, this process would only keep the location of the zero level set unchanged. This means the derivatives of ϕ cannot be computed directly from the level set function by differentiating the function ϕ itself after the regularization procedure. Therefore, to compute the derivatives of the level set function on the zero level set, we need to advect those derivatives as well. We first let $\xi = \phi_x$ and $\eta = \phi_\theta$. Differentiating the advection equation for ϕ with respect to x and θ , respectively, we have

$$(27) \quad \begin{aligned} \xi_z + u\xi_x + v\xi_\theta + u_x \xi + v_x \eta &= 0, \\ \eta_z + u\eta_x + v\eta_\theta + u_\theta \xi + v_\theta \eta &= 0. \end{aligned}$$

We might apply the same idea to the advection equation for takeoff angles as well so that the derivatives of takeoff angles could be determined. Once those ingredients are in place, the amplitude could be obtained. However, we will not use this approach because this is not efficient computationally and it is difficult to reconcile the accuracies of four different derivatives numerically.

Instead, defining

$$(28) \quad \Delta = \psi_x \phi_\theta - \psi_\theta \phi_x$$

and differentiating it with respect to z , we have the advection equation

$$(29) \quad \Delta_z + \nabla_{x,\theta} \cdot (\mathbf{u} \Delta) = 0,$$

and the amplitude can then be computed by

$$(30) \quad A(z; x, \theta) = \frac{1}{2\pi} \sqrt{\left| \frac{c}{2 \cos \theta} \frac{\Delta}{\phi_\theta} \right|}.$$

Therefore, we can simply solve the advection equations for ϕ_x , ϕ_θ and Δ in order to get the amplitude. We need the advection equation for ϕ_x because it is coupled with the one for ϕ_θ .

In general, Δ is a bounded quantity and ϕ_θ may approach zero. When ϕ_θ goes to zero, A goes to ∞ and we are approaching caustics.

Next we have to initialize the quantities that we are going to advect. At $z = 0$, we can set ϕ_x and ϕ_θ equal to 1 and 0, respectively. However, ψ_x is a singular function at the source and it is better to start computing ψ_x and ψ_θ at some $z = dz > 0$ close to zero. Assuming that the velocity c can be approximated by a constant near the source, we have

$$(31) \quad \begin{aligned} \psi_x(z, x, \theta)|_{z=dz} &= \frac{\cos^2 \theta}{dz}, \\ \psi_\theta(z, x, \theta)|_{z=dz} &= 1. \end{aligned}$$

Thus at small $z = dz > 0$,

$$(32) \quad \phi(z, x, \theta)|_{z=dz} = x - dz \tan \theta,$$

and $\Delta(dz, x, \theta) \equiv -2$, which is independent of the dz as long as the velocity can be well approximated by a constant near the source. This makes the computation of amplitude stable.

2.5. Caustics. Mathematically, caustic surfaces are envelopes of the family of rays. In the geometrical optics, at a caustic the amplitude of the asymptotic expansion becomes infinite, so that the usual asymptotic expansion is no longer valid at caustics, and some special expansions have been introduced to construct wave fields near the caustics [27, 6].

In the current level set formulation, the caustic curves correspond to

$$\{(z, x) : \phi(z, x, \theta(x, z)) = 0 \text{ and } \phi_\theta(z, x, \theta(x, z)) = 0\}.$$

On the zero level set, when $\phi_\theta \neq 0$, there exists local unique projection onto the x -space; when $\phi_\theta = 0$, the corresponding singularities or catastrophes of the implicit function $\theta = \theta(z, x)$ for fixed z 's are identified as caustics [43].

3. Implementation.

3.1. Local level set method. The computational complexity of the algorithm in [34] can be improved dramatically by implementing a narrow banding [1] or PDE-based version [32] of local level set method. In this work we adopt a version similar to the one proposed in [32].

Because we are interested only in the zero level set, all the updates can actually be done in a tube centered at $\phi = 0$. The radius of this tube, γ , is picked to be $5\Delta x$, due to the fact that five grid values are needed for the fifth order weighted essentially nonoscillatory (WENO) scheme when solving the advection equations. Therefore, by only considering the grid points within this tube, the complexity of the algorithm in [34] can be reduced by a factor of N from $O(N^3 \log N)$ to $O(N^2 \log N)$.

Reinitialization and orthogonalization are the two core ingredients in the local level set method as proposed in [32]. Reinitialization restores the equally spaced property for the level sets. The usual way is to make ϕ a signed distance function without moving the zero level set of ϕ appreciably. To achieve this, one can solve the following equation to steady state $\tilde{\phi}_\infty$ [38, 50, 9, 16, 32, 30]:

$$(33) \quad \frac{\partial \tilde{\phi}}{\partial \xi} + S(\phi)(|\nabla \tilde{\phi}| - 1) = 0$$

$$(34) \quad \tilde{\phi}|_{\xi=0} = \phi(z, \dots).$$

Here $S(\phi)$ could be the smoothed signum function [32]

$$(35) \quad S(\phi) = \frac{\phi}{\sqrt{\phi^2 + |\nabla \phi|^2 \Delta x \Delta \theta}},$$

where Δx and $\Delta \theta$ are the mesh sizes along x - and θ -directions, respectively. However, we usually only need to evolve equation (33) for a few steps. How often we should invoke the reinitialization step is a subtle issue; see [32, 30] for some discussions. Because we are only interested in the value of T where $\phi = 0$, we apply the following orthogonalization procedure [9, 16, 32, 30]:

$$(36) \quad \frac{\partial \hat{T}}{\partial \xi} + \text{sgn}(\phi) \left(\frac{\nabla \phi}{|\nabla \phi|} \cdot \nabla \hat{T} \right) = 0,$$

$$(37) \quad \hat{T}|_{\xi=0} = T(z, \dots)$$

which theoretically preserves the values of T where $\phi = 0$, but changes them elsewhere such that the new T does not vary too much near the desired region. At the steady state, $\nabla \phi \cdot \nabla \hat{T} = 0$.

3.2. Detecting caustics. Because passing through a caustic implies overturning of the zero level set in the x - θ space, the number of θ 's such that $\phi(z, x, \theta(x)) = 0$ will increase or decrease by two when x varies monotonically. Therefore, a simple way to detect caustics is first enumerating the number of roots θ_k 's for every x_i , then checking where those numbers have sudden jumps, and finally approximating locations of caustics by taking the midpoint of two adjacent x_i 's which have different numbers of θ_k . The resulting approximation of the caustics locations is of first-order accuracy.

Let x_c^* be the exact location of a caustic at some fixed z^* . Assume that x_c is the computed caustic location obtained from the level set formulation, i.e., solving

$$(38) \quad \phi(z^*, x, \theta(x, z^*)) = 0,$$

$$(39) \quad \phi_\theta(z^*, x, \theta(x, z^*)) = 0.$$

Let x'_c be the approximate caustic location computed using our midpoint approximation. We have at least $x_c = x_c^* + O(\Delta x^2)$ which is delivered by the second-order scheme used here. Because the distance between x_c and x'_c is less than $\Delta x/2$, we have $x'_c = x_c + O(\Delta x)$ and, therefore, $x'_c = x^* + O(\Delta x)$.

In terms of multivalued travel-times, passing through a caustic implies that the number of travel-times increases or decreases by two as we will see in numerical examples.

3.3. Algorithm. Hence we have the following local level set algorithm for computing the geometrical optics terms.

I. Initialization.

1. Given N_x and N_θ , determine

$$\Delta x = \frac{x_{\max} - x_{\min}}{N_z - 1} \text{ and } \Delta\theta = \frac{2\theta_{\max}}{N_\theta - 1}.$$

2. Initialize ϕ, T, ϕ_x and ϕ_θ at $z = 0$.
3. For each (x_i, θ_j) , where $i = 1, \dots, N_x$ and $j = 1, \dots, N_\theta$, check if any of $|\phi(x_i, \theta_j)|, |\phi(x_{i-1}, \theta_j)|, |\phi(x_{i+1}, \theta_j)|, |\phi(x_i, \theta_{j-1})|$ or $|\phi(x_i, \theta_{j+1})|$ is less than γ . Collect all these points and call the set Γ .

II. March in z until $z = z_{\max}$.

1. Determine Δz from the CFL condition.
2. March one Δz step by solving the level set equation (10) in Γ .
3. Reinitialize the level set function in Γ by solving (33).
4. March one Δz step by solving the travel-time equation (17) in Γ .
5. If $z \neq \Delta z$, update Δ by solving (29).
6. Orthogonalize T, ϕ_x and ϕ_θ to ϕ respectively in Γ by solving (36).
7. If $z \neq \Delta z$, orthogonalize Δ to ϕ in Γ . Otherwise, initialize Δ .
8. Update the tube Γ .
9. Detect caustics by checking if there is a change in the number of θ_k 's which gives $\phi(z; x_i, \theta_k) = 0$ for two adjacent x_i 's.

III. Output. For each x_i with $i = 1, \dots, N_x$,

1. Determine all root θ_k such that $\phi(z_{\max}; x_i, \theta_k) = 0$ ($k = 1, \dots$).
2. Determine $T(z_{\max}; x_i, \theta_k)$ ($k = 1, \dots$) by interpolation.
3. Determine $\phi_x(z_{\max}; x_i, \theta_k), \phi_\theta(z_{\max}; x_i, \theta_k)$ and $\Delta(z_{\max}; x_i, \theta_k)$ ($k = 1, \dots$) by interpolation, and then compute $A(z_{\max}; x_i, \theta_k)$.

To determine Δz in step II.1, we only need to scan through the grid points in the computational tube Γ in order to determine the maxima of velocity fields u and v , and this takes $O(N \log N)$ steps.

In step II, the level set equation and the travel-time equation are decoupled and can be solved separately. The spacial derivatives are approximated by a fifth-order WENO-Godunov scheme [22] while a third-order total variation diminishing-Runge-Kutta (TVD-RK) method [31] is used for the time marching.

Unlike the global level set method, the reinitialization step in II.3 is used not only to regularize the level set function but also to ensure the location of the tube in step II.8 more accurate. This step is necessary here and the number of iterations is to be determined so that the information of the location of the zero level set is propagated by a distance larger than γ , the radius of the tube. Numerically, one or two steps per iteration in z would be enough to get a reasonably good solution. However, formally, let β be the CFL number used in the reinitialization and m_{\min} be the minimum number of iterations of reinitialization; then we have

$$(40) \quad m_{\min} = \frac{\gamma}{\beta \min(\Delta x, \Delta \theta)}.$$

Because $\gamma = O(\Delta x)$, $m_{\min} = O(1)$. Overall the complexity of the reinitialization step for each Δz advancement would be equal to the number of grid points within the tube and is given by $O(N \log N)$.

For the root-finding and the interpolation in step III, we can simply use any nonoscillatory interpolation scheme, for example, linear interpolation or ENO reconstruction.

The next issue is how to update the computational tube Γ . A simple way is to scan all grid points in the domain and to apply the same procedure as that in I.3. The complexity of the resulting method will be $O(N^2)$. However, because the motion of the zero level set is purely advective, zeros will not be generated outside the tube. We can, therefore, update the tube by only scanning through the boundary of Γ , and this requires only $O(N \log N)$ operations.

As a result, for each iteration in z -direction, the complexity is $O(N \log N)$. Because of the CFL condition, the number of iterations in z is of $O(N)$. Overall the complexity of this algorithm is only $O(N^2 \log N)$. Comparing to $O(N^4)$ as typically seen in the Lagrangian ray tracing method, this Eulerian method is highly efficient and attractive.

4. Numerical examples. For the first three examples, we put a point source at the origin and velocity functions $c(x, z)$ are all C^∞ . The fourth example, the synthetic Marmousi model, is a very challenging one where the velocity function is given only as a gridded function. Unless specified, the computational domain we use in the following examples is chosen to be

$$(41) \quad \Omega_p = \{(x, \theta) : -1 \leq x \leq 1, \theta_{\max} \leq \theta \leq \theta_{\max}\},$$

where $\theta_{\max} = 9\pi/20$. Accordingly, the Marmousi velocity will be rescaled to the above computational domain.

4.1. Constant model. The simplest case one can imagine is the constant velocity model with $c(x, z) = 1$. Figure 1 shows the exact and computed travel-times and amplitudes of the constant model. The solid lines are the exact solutions. The numerical solutions match well with the true values.

Tables 1 and 2 show the convergence results for this test case. Convergence history for travel-time solutions is shown in Table 1, while Table 2 contains that of the amplitudes. The results show second-order convergence for both travel-time solution and amplitude at $x = 1$.

In this simple case, we can also compute the solution where we assume the boundary $x = x_{\max}$ is reflective. When the zero level set hits the boundary $x = x_{\max}$ in the $x - \theta$ space, it will not leave the domain; instead, a new ray will be generated in the

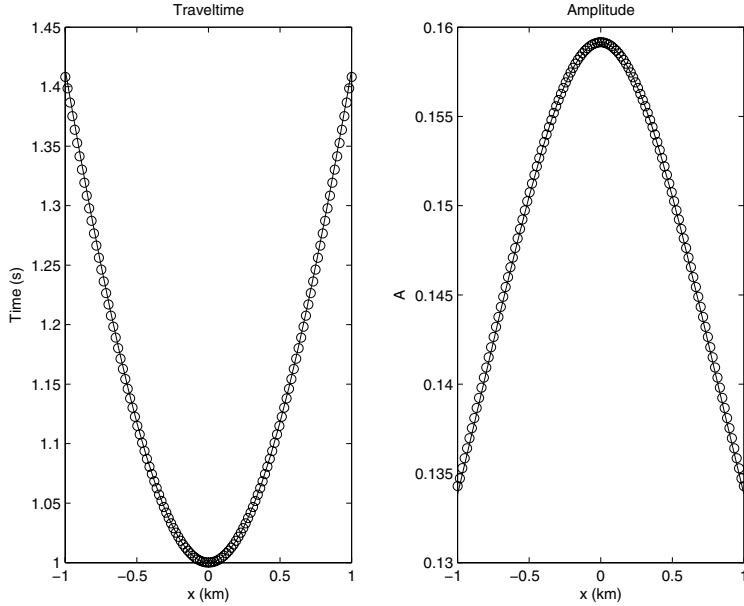


FIG. 1. (*Constant Model*) Travel-times and amplitudes at $z = 1$ (km) using a 120-by-120 grid. Solid line: the exact solution. Circles: the solution using the local level set method.

TABLE 1
(*Constant Model*) Accuracy and convergence order of travel-times at $z = 1$ km.

N_x	l_1 error	l_1 order	l_2 error	l_2 order	l_∞ error	l_∞ order
11	0.01044350		0.01077493		0.01504211	
21	0.00580110	0.8482	0.00540664	0.9948	0.00678677	1.1482
41	0.00193626	1.5830	0.00251217	1.5640	0.00251217	1.4337
81	0.00050419	1.9412	0.00047756	1.9369	0.00069198	1.8601
161	0.00011634	2.1156	0.00011220	2.0895	0.00017029	2.0227
321	0.00002791	2.0592	0.00002721	2.0435	0.00004292	1.9882

TABLE 2
(*Constant Model*) Accuracy and convergence order of amplitudes at $z = 1$ km.

N_x	l_1 error	l_1 order	l_2 error	l_2 order	l_∞ error	l_∞ order
11	0.00093010		0.00091941		0.00123784	
21	0.00052955	0.8126	0.00049836	0.8835	0.00061722	1.0039
41	0.00016404	1.6907	0.00015484	1.6863	0.00020976	1.5570
81	0.00004076	2.0086	0.00003870	2.0000	0.00005544	1.9195
161	0.00000970	2.0709	0.00000930	2.0568	0.00001391	1.9944
321	0.00000261	1.8924	0.00000253	1.8735	0.00000382	1.8623

computational space at the same $x = x_{\max}$ and with θ having opposite sign to the original ray.

For the travel-time, we have to determine boundary conditions for the incident and the reflected rays separately. We can use the same boundary condition as in the nonreflective case for the incident ray. The reflective ray has the same travel-time as the incident ray at the boundary $x = x_{\max}$.

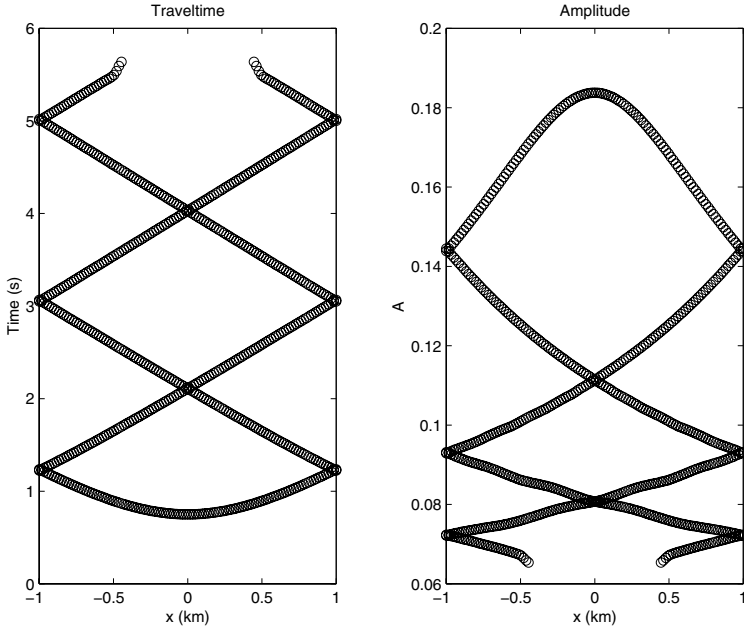


FIG. 2. (*Constant Model*) Travel-time at $z = 0.75\text{km}$ with reflective boundary conditions.

Therefore, we have the following boundary condition on $x = x_{\max}$:

$$(42) \quad \begin{aligned} \phi(x_{\max}, \theta) &= \phi(x_{\max}, -\theta) \\ \phi_x(x_{\max}, \theta) &= \phi_x(x_{\max}, -\theta) \\ \phi_\theta(x_{\max}, \theta) &= \phi_\theta(x_{\max}, -\theta) \\ \Delta(x_{\max}, \theta) &= \Delta(x_{\max}, -\theta) \\ T(x_{\max}, \theta) &= \begin{cases} \text{from (19)} & \text{if } u(x_{\max}, \theta) > 0 \\ T(x_{\max}, -\theta) & \text{if } u(x_{\max}, \theta) < 0 \end{cases} \end{aligned}$$

Similar boundary conditions can be used on the other side $x = x_{\min}$ and will not be fully discussed here. For the other two boundaries $\theta = \theta_{\max}$ and $\theta = -\theta_{\max}$, we can use the same boundary conditions as in the nonreflective case detailed in section 2.

Figure 2 shows the solutions obtained at $z = 1\text{km}$ using the proposed method with reflective boundary conditions imposed on both boundaries $x = \pm 1$; multiple reflections are captured clearly as shown in travel-times and amplitudes using 120 grid points in both x - and θ -directions.

4.2. Waveguide model. The velocity function is given by

$$(43) \quad c(x, z) = 1.1 - \exp(-0.5x^2).$$

The function is symmetric with respect to $x = 0$, and we also expect the same type of symmetry in both the travel-time and the amplitude.

Figure 3 shows travel-times, amplitudes and some intermediate quantities at $z = 1.6\text{km}$ using 240-by-240 grid points, respectively. The solid lines in the travel-time and amplitude plots are obtained using a ray tracing method. The solutions are symmetric as expected. Δ in this velocity model should be equal to -2 everywhere.

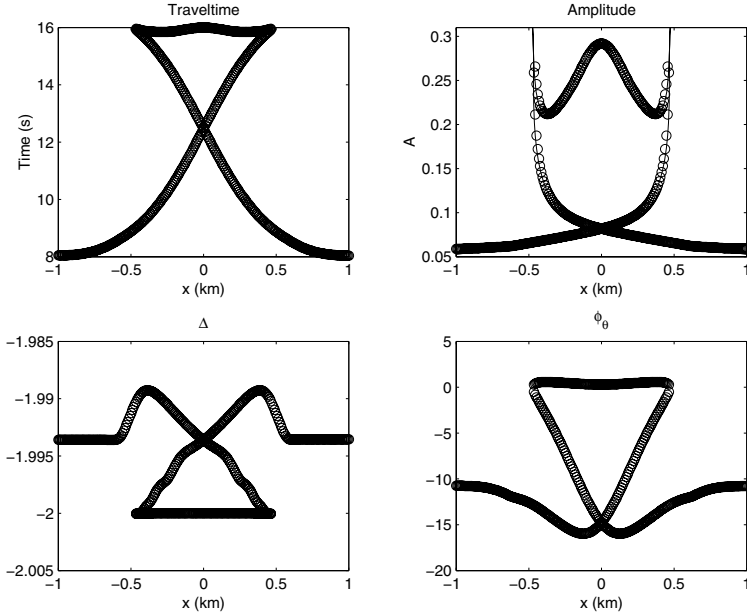


FIG. 3. (Waveguide Model) Travel-time, amplitude, Δ and ϕ_θ at $z = 1.6\text{km}$ using a 240-by-240 grid.

As we mentioned earlier, the velocity model is approximated by a constant near the source and this gives the initial condition $\Delta = -2$ at $z = dz$. For this waveguide model, because $u_x = v_\theta = 0$, the equation for Δ is purely advective; therefore the exact solution is $\Delta(z; x, \theta) = -2$, which is independent of z . The variations in the subplot of Δ in Figure 3 are due to numerical errors.

The singularities in the amplitudes, shown in the upper right subplot in Figure 3, come from the vanishing of ϕ_θ on the zero level set of ϕ at around $x = \pm 0.45\text{km}$, shown in the lower right subplot in Figure 3.

The caustic curves detected by the local level set method are shown in Figure 4: circles are computed locations of the caustics in the waveguide model, and the solid lines are the rays emanating from the source by a ray tracing method. The caustic locations are exactly those places where rays form an envelope as seen in the figure.

To demonstrate the improvement in the computational efficiency of the current formulation, we computed the solutions of this test case on a Pentium IV desktop with different sets of grid points and recorded the computational time. Table 3 shows the dramatic improvement delivered by the $O(N^2 \log N)$ local level set method proposed here and the typical behavior of $O(N^3 \log N)$ complexity offered by the global level set method.

4.3. Sinusoidal model. This example is adapted from the sinusoidal waveguide model used in [40, 41], and the velocity function is given by

$$(44) \quad c(x, z) = 1 + 0.2 \sin(0.5\pi z) \sin[3\pi(x + 0.55)].$$

Figure 5 shows travel-times, amplitudes and some intermediate quantities at $z = 2.0\text{km}$ using 240-by-240 grid points. The subplot for travel-times in Figure 5 shows that the triplications in the travel-time developed at $z = 2.0$ are clearly captured by the level set Eulerian method. Singularities in the amplitude come from the

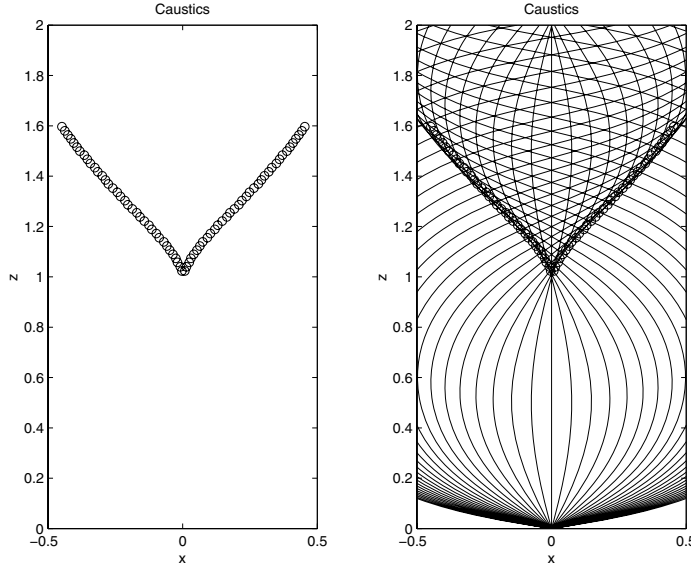


FIG. 4. (Waveguide Model) Location of caustics and some rays from a ray tracing method. Caustics are determined by the local level set method with a 360-by-360 grid in the $x\theta$ space.

TABLE 3

(Waveguide Model) Time comparison for global and local level set methods: evolving up to $z = 1.6$.

Grid	Global: minutes	Local: minutes
120×120	72	8
240×240	641	19
480×480	5439	58

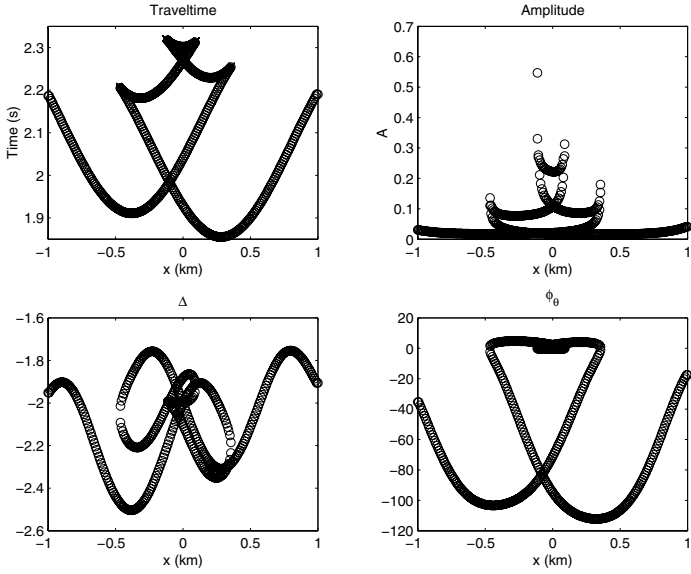


FIG. 5. (Sinusoidal Model) Travel-time, amplitude, Δ and ϕ_θ at $z = 2.0\text{km}$ using a 240-by-240 grid.

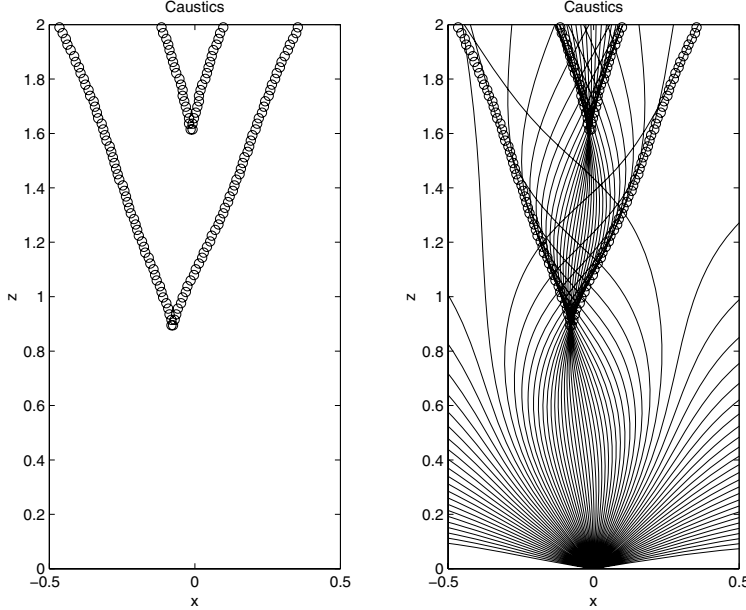


FIG. 6. (*Sinusoidal Model*) Location of caustics and some rays from a ray tracing method. Caustics are determined by the local level set method with a 360-by-360 grid in the x - θ space.

overturning of the zero level set in the phase space, i.e., $\phi_\theta = 0$, which is shown in the lower right subfigure in Figure 5.

Figure 6 shows locations of the caustics detected by the proposed method, and the results match those from the ray tracing method.

4.4. Synthetic Marmousi model. This example is the Marmousi model from the 1996 INRIA Workshop on Multi-arrival Travel-times. The calibration data used here were computed by Dr. Klimes and can be found at <http://www.caam.rice.edu/~benamou/traveltimes.html>. This is a synthetic model which will challenge the level set method used here.

The original Marmousi model is sampled on a 24m-by-24m grid, consisting of 384 samples in the x -direction and 122 samples in the z -direction; therefore the model dimension is 9.192km long in the x -direction and 2.904km deep in the z -direction. In the computational results presented here, we use a portion of Marmousi model, i.e., a window from 2.64km to 9.36km in the x -direction and from 0km to 2.904km in the z -direction. The source is located at $x=6.0\text{km}$ and $z=2.8\text{km}$. The purpose is to compute (possibly multivalued) travel-times for those sampling points, i.e., the receivers from 160 to 340 on the surface $z=0.0\text{km}$. It should be emphasized that since we are using a local level set method, we can choose such a large window of the velocity model. In the example presented in [34], we were able to deal with a much smaller portion of the velocity model because we used a global level set method.

As illustrated in [34], to resolve a complicated wave front like the one generated by the Marmousi model, we have to use very fine computational meshes which need huge memory storage in the global level set setup. In the previous work [34], we applied up to 400 grid points in the x -direction to resolve the solutions between receiver 200 to 300. With the local level set method developed here, we are able to tackle a much

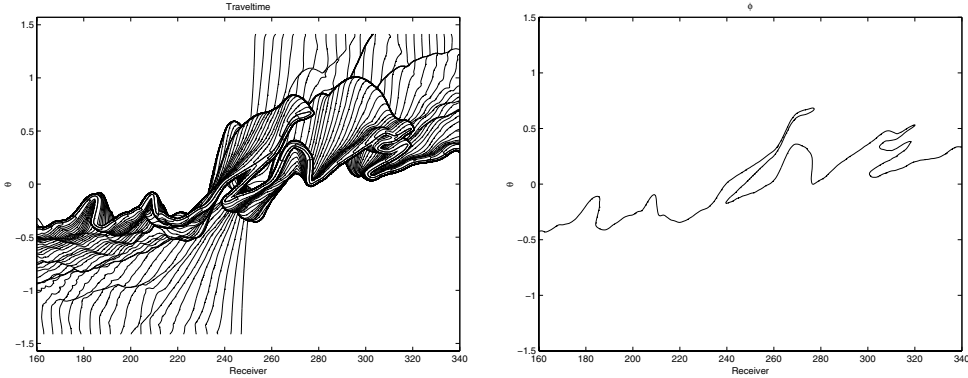


FIG. 7. (Marmousi Model) Contours of the travel-time and the zero level set at $z = 0.0\text{km}$.

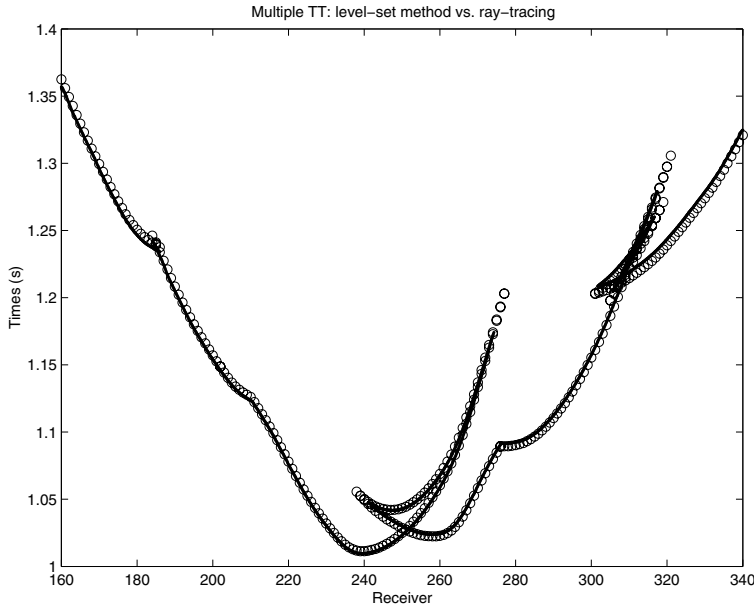


FIG. 8. (Marmousi Model) Comparison between travel-times using a ray tracing method and the local level set method at $z = 0.0\text{km}$.

larger portion of the original velocity and produce higher resolution travel-times with reasonable memory and computational cost. Figure 7 shows the zero level set and its overlay on the travel-time field by using a refinement of the original model with a refinement ratio = 8, i.e., we are using 1440 grid points in the x -direction to resolve the arrivals between receiver 160 to 340. As we can see from the plot, the zero level set has lots of overturnings and tiny tips. Therefore, there are lots of caustics developed in the wave propagation. The resulting travel-times at the surface along with the ray tracing solutions are shown in Figure 8; the two solutions match with each other reasonably well. Near receiver 340 we have captured five branches of travel-times as shown in Figure 9.

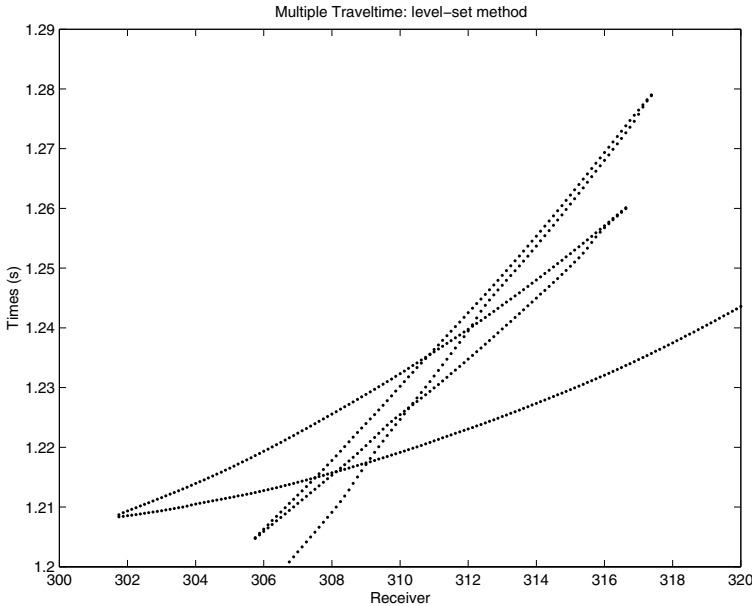


FIG. 9. (*Marmousi Model*) Zoom-in at receiver 310: the local level set method at $z = 0.0\text{km}$.

5. Conclusion. We have proposed a local level set method for paraxial geometrical optics, so that the multivalued travel-time and amplitude can be constructed with ease. The computational complexity of the algorithm is $O(N^2\log N)$, therefore it is highly efficient. Although the subhorizontal condition is required for the approach to work, it is suitable for many applications, such as reflection seismics, underwater acoustics and optics. The future work includes grafting this approach to high resolution seismic inversion [39] and computing the high frequency wave field using a time domain approach proposed in [6] rather than the usual frequency domain approach in [27].

Acknowledgment. J. Qian thanks Professors R. Burridge, S. Osher, F. Reitich and W. W. Symes for helpful discussions. This work was supported by ONR grant N00014-02-1-0720. J. Qian was partially supported by NSF DMS-0542174.

REFERENCES

- [1] D. ADALSTEINSSON AND J. A. SETHIAN, *A fast level set method for propagating interfaces*, *J. Comput. Phys.*, 118 (1995), pp. 269–277.
- [2] J.-D. BENAMOU, *Direct solution of multi-valued phase-space solutions for Hamilton–Jacobi equations*, *Comm. Pure Appl. Math.*, 52 (1999), pp. 1443–1475.
- [3] J. D. BENAMOU, *An introduction to Eulerian geometrical optics (1992–2002)*, *J. Sci. Comput.*, 19 (2003), pp. 63–93.
- [4] J.-D. BENAMOU AND I. SOLLIEC, *A Eulerian method for capturing caustics*, *J. Comput. Phys.*, 162 (2000), pp. 132–163.
- [5] M. BORN AND E. WOLF, *Principles of Optics*, Macmillan, New York, 1964.
- [6] R. BURRIDGE, *Asymptotic evaluation of integrals related to time-dependent fields near caustics*, *SIAM J. Appl. Math.*, 55 (1995), pp. 390–409.
- [7] R. BURRIDGE, M. V. DE HOOP, D. MILLER, AND C. SPENCER, *Multiparameter inversion in anisotropic media*, *Geophys. J. Internat.*, 134 (1998), pp. 757–777.

- [8] V. CERVENY, I. A. MOLOTKOV, AND I. PSENICK, *Ray Method in Seismology*, Univerzita Karlova Press, Praha, Czech Republic, 1977.
- [9] S. CHEN, B. MERRIMAN, S. OSHER, AND P. SMEREKA, *A simple level set method for solving Stefan problems*, J. Comput. Phys., 135 (1997), pp. 8–29.
- [10] L.-T. CHENG, H. LIU, AND S. J. OSHER, *High Frequency Wave Propagation in Schrodinger Equations Using the Level Set Method*, preprint 2003; available online at www.levelset.com.
- [11] M. G. CRANDALL AND P. L. LIONS, *Viscosity solutions of Hamilton–Jacobi equations*, Trans. Amer. Math. Soc., 277 (1983), pp. 1–42.
- [12] B. ENGQUIST AND O. RUNBORG, *Multi-phase computations in geometrical optics*, J. Comput. Appl. Math., 74 (1996), pp. 175–192.
- [13] B. ENGQUIST AND O. RUNBORG, *Computational high frequency wave propagation*, Acta Numer., 12 (2003), pp. 181–266.
- [14] B. ENGQUIST, O. RUNBORG, AND A-K TORNBERG, *High frequency wave propagation by the segment projection method*, J. Comput. Phys., 178 (2002), pp. 373–390.
- [15] L. C. EVANS, *Towards a quantum analogue of weak KAM theory*, Comm. Math. Phys., 244 (2004), pp. 311–334.
- [16] R. FEDKIW, T. ASLAM, B. MERRIMAN, AND S. OSHER, *A non-oscillatory Eulerian approach to interfaces in multimaterial flows (the ghost fluid method)*, J. Comput. Phys., 152 (1999), pp. 457–492.
- [17] S. FOMEL AND J. SETHIAN, *Fast phase space computation of multiple traveltimes*, Proc. Natl. Acad. Sci., 99 (2002), pp. 7329–7334.
- [18] S. GEOLTRAIN AND J. BRAC, *Can we image complex structures with first-arrival traveltimes*, Geophys., 58 (1993), pp. 564–575.
- [19] L. GOSSE, *Using K-branch entropy solutions for multivalued geometric optics computations*, J. Comput. Phys., 180 (2002), pp. 155–182.
- [20] L. GOSSE AND P. A. MARKOWICH, *Multiphase semiclassical approximations of an electron in a one-dimensional crystalline lattice*, J. Comput. Phys., 197 (2004), pp. 387–417.
- [21] S. GRAY AND W. MAY, *Kirchhoff migration using eikonal equation traveltimes*, Geophys., 59 (1994), pp. 810–817.
- [22] G. S. JIANG AND D. PENG, *Weighted ENO schemes for Hamilton–Jacobi equations*, SIAM J. Sci. Comput., 21 (2000), pp. 2126–2143.
- [23] S. JIN AND X. LI, *Multi-phase computations of the semi-classical limit of the Schrodinger equation and related problems*, Phys. D, 182 (2003), pp. 46–85.
- [24] S. JIN AND S. OSHER, *A Level Set Method for the Computation of Multivalued Solutions to Quasi-linear Hyperbolic PDEs and Hamilton–Jacobi Equations*, preprint 2003; available online at www.levelset.com.
- [25] J. B. KELLER AND R. M. LEWIS, *Asymptotic methods for partial differential equations: The reduced wave equation and Maxwell's equations*, Surv. Appl. Math., 1 (1995), pp. 1–82.
- [26] P. L. LIONS, *Generalized Solutions of Hamilton–Jacobi Equations*, Pitman, Boston, 1982.
- [27] D. LUDWIG, *Uniform asymptotic expansions at a caustic*, Comm. Pure Appl. Math., XIX (1966), pp. 215–250.
- [28] S. OPERTO, S. XU, AND G. LAMBARE, *Can we image quantitatively complex models with rays*, Geophys., 65 (2000), pp. 1223–1238.
- [29] S. OSHER, L.-T. CHENG, M. KANG, H. SHIM, AND Y-H TSAI, *Geometric optics in a phase space based level set and Eulerian framework*, J. Comput. Phys., 179 (2002), pp. 622–648.
- [30] S. OSHER AND R. P. FEDKIW, *Level Set Methods and Dynamic Implicit Surfaces*, Springer-Verlag, New York, 2003.
- [31] S. J. OSHER AND C. W. SHU, *High-order essentially nonoscillatory schemes for Hamilton–Jacobi equations*, SIAM J. Numer. Anal., 28 (1991), pp. 907–922.
- [32] D. PENG, B. MERRIMAN, S. OSHER, H. K. ZHAO, AND M. KANG, *A pde-based fast local level set method*, J. Comput. Phys., 155 (1999), pp. 410–438.
- [33] J. QIAN, L.-T. CHENG, AND S. J. OSHER, *A level set based Eulerian approach for anisotropic wave propagations*, Wave Motion, 37 (2003), pp. 365–379.
- [34] J. QIAN AND S. LEUNG, *A level set method for paraxial multivalued traveltimes*, J. Comput. Phys., 197 (2004), pp. 711–736.
- [35] J. QIAN AND W. W. SYMES, *Adaptive finite difference method for traveltime and amplitude*, Geophys., 67 (2002), pp. 167–176.
- [36] S. J. RUUTH, B. MERRIMAN, AND S. J. OSHER, *A fixed grid method for capturing the motion of self-intersecting interfaces and related PDEs*, J. Comput. Phys., 151 (1999), pp. 836–861.
- [37] J. STEINHOFF, M. FAN, AND L. WANG, *A new Eulerian method for the computation of propagating short acoustic and electromagnetic pulses*, J. Comput. Phys., 157 (2000), pp. 683–706.
- [38] M. SUSSMAN, P. SMEREKA, AND S. J. OSHER, *A level set approach for computing solutions to incompressible two-phase flows*, J. Comput. Phys., 114 (1994), pp. 146–159.

- [39] W. W. SYMES, *Mathematics of Reflection Seismology*, Annual Report, The Rice Inversion Project, Rice University, Houston, TX, 1995; also available online from <http://www.trip.caam.rice.edu/>.
- [40] W. W. SYMES, *A slowness matching finite difference method for traveltimes beyond transmission caustics*, Expanded Abstracts, in the 68th Annual International Meeting, Society of Exploration Geophysicists, 1998, pp. 1945–1948.
- [41] W. W. SYMES AND J. QIAN, *A slowness matching Eulerian method for multivalued solutions of eikonal equations*, J. Sci. Comput., 19 (2003), pp. 501–526.
- [42] W. W. SYMES, R. VERSTEEG, A. SEI, AND Q. H. TRAN, *Kirchhoff Simulation, Migration and Inversion Using Finite Difference Traveltimes and Amplitudes*, Annual Report, The Rice Inversion Project, Rice University, Houston, TX, 1994; also available online from <http://www.trip.caam.rice.edu/>.
- [43] R. THOM, *Structural Stability and Morphogenesis*, Benjamin, New York, 1975.
- [44] J. VAN TRIER AND W. W. SYMES, *Upwind finite-difference calculation of traveltimes*, Geophys., 56 (1991), pp. 812–821.
- [45] J. VIDALE, *Finite-difference calculation of travel times*, Bull. Seismol. Soc. Amer., 78 (1988), pp. 2062–2076.
- [46] V. VINJE, E. IVERSEN, AND H. GJYSTDAL, *Travelttime and amplitude estimation using wavefront construction*, Geophys., 58 (1993), pp. 1157–1166.
- [47] B. S. WHITE, *The stochastic caustic*, SIAM J. Appl. Math., 44 (1984), pp. 127–149.
- [48] B. S. WHITE, *Wave action on currents with vorticity*, J. Fluid Mech., 386 (1999), pp. 329–344.
- [49] L. ZHANG, *Imaging by the wavefront propagation method*, Ph.D. thesis, Stanford University, Stanford, CA 94305, 1993.
- [50] H.-K. ZHAO, T. CHAN, B. MERRIMAN, AND S. J. OSHER, *A variational level set approach for multiphase motion*, J. Comput. Phys., 127 (1996), pp. 179–195.